Energy & Buildings 166 (2018) 477–488

Contents lists available at ScienceDirect

Energy & Buildings

journal homepage: www.elsevier.com/locate/enbuild

Fault detection and diagnosis for nonlinear systems: A new adaptive Gaussian mixture modeling approach

Majid Karami, Liping Wang*

Civil and Architectural Engineering Department, University of Wyoming, Laramie, WY, United States

ARTICLE INFO

Article history:
Received 3 August 2017
Revised 5 February 2018
Accepted 14 February 2018
Available online 21 February 2018

Keywords:
Gaussian mixture model
Unscented Kalman filter
Multi-chiller plant
Fault detection and diagnosis

ABSTRACT

In heating, ventilation and air-conditioning (HVAC) systems, early detection and diagnosis of faults are of critical importance to save energy and improve the performance of system components. The challenge is developing an automatic fault detection and diagnosis algorithm for monitoring of multi-mode nonlinear systems. This paper proposes a novel adaptive Gaussian mixture model (AGMM) approach for automatic fault detection and diagnosis in nonlinear systems. The concept of this method relies on developing a time-varying probabilistic machine-learning model for non-linear systems. In this study, Gaussian mixture model regression (GMMR) technique is used to model a nonlinear system based on measurement data. Unscented Kalman filter (UKF) is then integrated with GMMR for adjusting the model parameters based on the feedback of residuals between observation and model prediction. The proposed algorithm is able to detect and diagnose simultaneous faults in systems from monitoring variations of key GMMR parameters. The application of AGMM method is demonstrated for detection and diagnosis of common faults in a water-cooled multi-chiller plant system. Faults including energy efficiency degradation in chillers were tested with the proposed method. Results indicate that the AGMM approach is successful in detection and diagnosis of simultaneous faults.

1. Introduction

Heating, ventilation and air conditioning (HVAC) systems are major sources of energy consumption in buildings. Abnormal operation of HVAC components can lead to significant waste of energy, around 15–30% of the energy used in buildings [1], equipment degradation and occupants discomfort. Automatic fault detection and diagnosis (AFDD) can save energy and avoid further system components degradation. Development of AFDD algorithm has been studied for a variety of dynamic systems. A comprehensive review of different AFDD methods has been accomplished for engineering process in general [2–4] and for building systems in specific [1,5].

1.1. Data-driven modeling

Analyzing big data, collected from complex systems, demands accurate and reliable models and flexible frameworks. Data-driven modeling technique attracts significant attention in system analysis, fault detection and industrial control. The main advantage of data-driven modeling approach is the reduced time and effort in developing system model.

Partial least square method (PLS) and principal component analysis (PCA) are of widely used methods to derive statistical models for dynamic systems. These methods assume a normal distribution of data which is not realistic in complex systems [6]. Gaussian mixture modeling (GMM) approach relaxes this restriction by enabling the estimation of complex densities. GMM uses unsupervised learning approach to partition the data into several clusters. Each cluster of data is approximated by a Gaussian distribution, known as mixture component, with its own mean and covariance. Then GMM provides a probabilistic model for complex densities by superposition of Gaussian distributions [7]. GMM can be extended to Gaussian mixture model regression (GMMR) form to generate a regression function between input and output data. GMMR creates a local regression function for each component of GMM and then approximate the correlation between input and output data by weighted sum of local regressions [8]. Application of GMM and GMMR has been extended to model a variety of dynamical systems.

GMMR has been employed as a data-driven model to predict air mass in spark-ignition combustion engine [9]. The result indicates that accuracy of GMMR outperforms local linear tree algorithm. Lan et al. [10] used GMM to estimate aircraft motion param-

* Corresponding author.
E-mail address: lwang12@uwyo.edu (L. Wang).

https://doi.org/10.1016/j.enbuild.2018.02.032
0378-7788/

eters. In this research, GMM has been combined with the Kalman filter to approximate the nonlinear multi-input multi-output dynamic of aircraft motion. In training process, a GMM is used to cluster the system input data and a Kalman filter is used to estimate the parameters of the linear model associated with each cluster. GMMR approach has been used in constructing virtual sensors for monitoring of parameters which are hard to be directly measured [11,12]. GMMR has also been used for prediction in other disciplines such as continuous tool wear prediction in milling process [13], learning robot motion [14,15], and human pose estimation [16].

To improve model accuracy, various methods have been proposed to update the GMM parameters when new observations become available. An incremental GMM estimation approach can be used to perform near-online mixture model clustering [17]. In this method, Expected Maximization algorithm is applied to a batch of newly arrived data and associated GMM is estimated. New GMM is merged to model extracted from the previous batch of data. Kristan et al. [18] proposed Kernel Density Estimation (KDE) approach which allows estimating probability density function, given new observation. Online Expected Maximization is another method proposed to recursively estimate the parameters of the data model with no requirement to store and use history of data [19].

Our approach proposed in this paper is called unscented Kalman filter (UKF) - Gaussian mixture model regression (GMMR). This method is used to develop baselines for system performance. Then, we update the parameters of GMMR model base on the feedback of error between observation and model prediction. The UKF is employed as an online parameter estimator [20].

1.2. Fault detection and diagnosis

Data-driven methods incorporating machine learning techniques have been used extensively in fault detection and diagnosis of HVAC systems. Most applied machine learning methods for AFDD of HVAC systems include, Bayesian probabilistic network model [21–23], support vector machine (SVM) [24,25], principal component analysis (PCA) [26,27], linear discriminant analysis (LDA) [28], tree structure learning [29], and fuzzy logic [30,31].

Application of GMM approach for fault detection and diagnosis intent has been motivated in various researches. GMM has been used to detect and diagnose faults in chemical processes based on reduced data subspace obtained by PCA and discriminate analysis [6]. This method requires developing GMM for each faulty mode. Another approach develops GMM from measurement variables and defines an index for each variable which shows the associated contribution to process fault [32,33]. We propose new approach toward extending Gaussian mixture clustering method to fault detection and diagnosis application. Instead of analyzing the faults in measurement space, we detect and diagnose system faults by monitoring and analysis of UKF-GMMR time-varying parameters.

In the context of fault detection and diagnosis in chiller plants, a few studies have been focused on common faults in chiller plant. Bonvini et al. [34] proposed a robust online AFDD method to detect and diagnose faults in chiller using nonlinear state estimation techniques. The FDD algorithm is based on a physical model of chiller which includes a parameter or state variable corresponding to each fault. The unscented Kalman filter with a back-smoothing method is used to estimate the parameters or states associated with different faults including chiller performance degradation fault, occlusion in condenser and evaporator valves, and sensor faults. Application of regression modeling for fault detection in chiller plants has been proposed in [35]. In this paper, fault detection and diagnosis of system level faults in various subsystems including cooling tower, chiller, pumps, and heat exchanger system has been studied. Each subsystem is characterized using one or several performance indices. Regression approach is used to model each performance index in fault-free conditions. The residuals between calculated and monitored performance indices are compared with associated adaptive thresholds to determine the status of each subsystem. For the chiller system, coefficient of performance and power consumption are used as performance indices. Regression models for chiller performance indices include chilled supply water temperature, entering condenser water temperature, and cooling load as driving variables. Hu et al. [36] employed multivariate GMM as a classification technique to detect chiller performance degradation fault. Three Gaussian mixture models have been created for a chiller in three modes of operations, fault free, moderate fault and sever fault. Then, given new observation, membership to predefined operational modes was computed. The application of GMM for AFDD in this study is limited by the need of creating a GMM for each faulty operations. Several models have to be generated for diagnosing common faults in the system of interests. In addition, the GMMs for AFDD do not change with time.

In this study, developing an adaptive model for detection and diagnosis of faults in a multi-chiller plant using system level data is explored. We created an AGMM approach. In this approach, 1) UKF-GMMR will capture both nonlinearities and time-varying properties of complex systems to create one baseline model representing fault-free operation; and 2) time-varying parameters in the GMMR model, reacting to the emergence of different faults, exhibit distinct patterns.

The proposed approach is aimed at reducing modeling effort by only developing a data-driven UKF-GMMR model for the fault-free operation. In addition, this approach provides single model to simulate all modes of operation and detect fault in individual chillers. Developing a regression model for performance index requires evaluating several models with various orders and cross terms [37]. Benefitting from unsupervised learning approach, the UKF-GMMR algorithm automatically determines the model structure along with the correlation between features.

The paper is presented in the structure as follows. We first introduce our proposed fault detection and diagnosis framework. Then, we formulate Gaussian mixture density estimation using K-means and EM method and we use mixture density to derive GMMR function. After that, we integrate UKF with GMMR to improve prediction accuracy. Finally, we discuss fault detection and diagnosis results using a multi-chiller plant as a case study based on the proposed new AGMM approach.

2. Fault detection and diagnosis methodology

Our proposed fault detection and diagnosis algorithm relies on the accurate time-varying GMMR of nonlinear systems representing design intent and classification of abnormal changes in key parameters of GMMR. Direct analysis of output residuals is mapped to the analysis of variation in GMMR parameters. Fig. 1 shows a general schematic of proposed AGMM method for fault detection and diagnosis.

Procedure to apply the AGMM method for fault detection and diagnostics is as follows.

1) Determine faults and associated characteristics (fault dynamic, severity).
2) Select appropriate sensors to acquire input-output data which is well-correlated to fault under study.
3) Collect fault free training data or simulate the system physical model under fault free condition in training time period.
4) Construct GMMR from training data
5) Integrate UKF into GMMR and run the model using fault free data to extract normal bound of variation for Gaussian mixture model parameters.

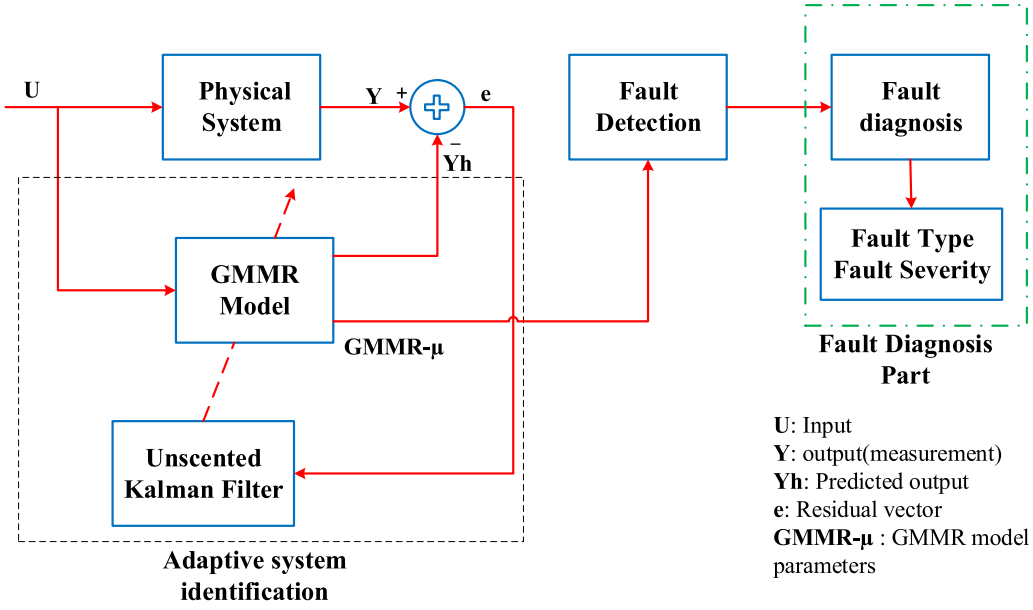

Fig. 1. Framework for fault detection and diagnosis using AGMM approach.

6) Collect faulty data or simulate the system physical model when each fault is created separately and store input-output data.
7) Run UKF-GMMR using faulty data and extract the pattern of change in GMM parameters for detection and diagnosis rules.
8) Test the framework using testing faulty data.

A detailed explanation of each component in the framework shown in Fig. 1 is as follows.

GMMR model: GMM is an unsupervised learning approach which frames system input and output information to a number of clusters. Each cluster is approximated by a Gaussian distribution characterized by a mean as the center of the cluster and a variance. The basic concept of GMMR is the piecewise approximation of a nonlinear function with the sum of weighted linear regression models. The parameters of each linear regression model are made up of clusters features. Since probabilistic features of real-world data set are hard to be described by a single distribution function, superposition of several sub-distribution functions can help to formulate complex densities. Detail equations for GMMR model are described in Section 3.

Unscented Kalman filter: The properties of the dynamic system vary when a fault occurs. Therefore, static GMMR is unable to track the system output under new circumstances. UKF as an adaption algorithm is integrated to GMMR to reconcile GMMR parameters in response to the error between observed output and model prediction. The centers of clusters associated with output data are considered as time-varying parameters in UKF-GMMR modeling structure. Detail equations for UKF-GMMR model are described in Section 4.

Fault detection: The centers of output clusters as parameters of GMMR are subject to change when the model tries to adaptively track the system behavior. When there is no fault in system, variations of GMMR parameters are limited to a normal bound. Normal thresholds associated with each time-varying parameters are extracted from training fault-free data. Fault occurrence creates abnormal change in model parameters leading to violating the normal thresholds and flagging fault alarm.

Fault diagnosis: Depending on fault type, change in parameters can arise abruptly or grow over time. This change is due to the unique structure of proposed GMMR, which decomposes the dynamic of a system to different clusters and therefore, faulty operation of a specific subcomponent of the system can be correlated to change in specific clusters. By recognizing the variation pattern of parameters, when different artificial known faults are imposed to a system, a set of rules can be elicited to diagnose the faults. Using proposed UKF-GMMR and extracted rules, it is possible to identify different faults even they happen simultaneously.

The proposed AFDD approach is computationally efficient. Therefore, it is feasible to implement the new AFDD algorithms in the real system application. GMMR will first be developed to represent healthy data as baselines for nonlinear systems. UKF will then be integrated with the GMMR model.

3. GMMR

3.1. GMM

Given N observations of input-output dataset $\boldsymbol{d_n} = [\boldsymbol{x_n}, y_n]^{\mathbb{T}} (n = 1 : N)$, where $\boldsymbol{x_n} \epsilon \mathbb{R}^{L\times 1}$ is input vector and $y_n \epsilon \mathbb{R}$ is output data, the joint density function of $(\boldsymbol{x}, y)$ can be written as a mixture of k Gaussian distributions as shown in Eq. (1). So, the probabilistic features of data are divided into the number of Gaussian mixtures k, weight coefficients π_j, mean $\boldsymbol{\mu_j}$ and covariance δ_j of each Gaussian component [8].

$$f(\boldsymbol{x}, y|\pi, \boldsymbol{\mu}, \delta) = \sum_{j=1}^{k} \pi_j N(\boldsymbol{x}, y|\boldsymbol{\mu_j}, \delta_j) \tag{1}$$

where

$$\sum_{j=1}^{k} \pi_j = 1, \quad \boldsymbol{\mu_j} = \begin{bmatrix} \boldsymbol{\mu_{jx}} \\ \mu_{jy} \end{bmatrix}, \quad \delta_j = \begin{bmatrix} \delta_{jxx} & \delta_{jxy} \\ \delta_{jyx} & \delta_{jyy} \end{bmatrix} \tag{2}$$

In Eq. (3) for a L-dimensional input vector $\boldsymbol{x}$ and 1-dimensional output vector y, $N(\boldsymbol{x}, y|\boldsymbol{\mu_j}, \delta_j)$ is multi-variable Gaussian probability distribution function.

$$N\left(\boldsymbol{x}, y|\boldsymbol{\mu_j}, \delta_j\right) = \frac{1}{(2\pi)^{(L+1)/2}} \frac{1}{\left|\delta_j\right|^{1/2}} \times \exp\left\{-\frac{1}{2}\left(\boldsymbol{d} - \boldsymbol{\mu_j}\right)^{\mathbb{T}} \delta_j{}^{-1} \left(\boldsymbol{d} - \boldsymbol{\mu_j}\right)\right\} \tag{3}$$

One solution to finding the unknown parameters of mixture model $(\pi_j, \boldsymbol{\mu_j}, \delta_j)$ is maximizing likelihood function of the mix-

ture model. Eq. (4) represents the log of the likelihood function for GMM. The likelihood is an index which reveals how well the model fits the given set of data.

$$\ln f(\boldsymbol{x}, y|\pi,\ \boldsymbol{\mu}, \delta) = \sum_{n=1}^{N} ln \sum_{j=1}^{k} \pi_j N(\boldsymbol{d_n}|\boldsymbol{\mu_j}, \delta_j) \tag{4}$$

Maximum likelihood solution cannot be obtained through closed-form analytical approach. Expected Maximization (EM) algorithm, as a numerical iterative optimization method, recognizes the value of model parameters which maximizes the likelihood function. Appendix A provides more details about the EM algorithm for determining the parameters of the GMM.

3.2. GMMR

Gaussian mixture probability function shown in Eq. (1) can be partitioned as function presented in Eq. (5).

$$\begin{aligned} f(\boldsymbol{x}, y|\pi, \boldsymbol{\mu}, \delta) &= \sum_{j=1}^{k} \pi_j N(y|\boldsymbol{x}, m_j(\boldsymbol{x}), \tau_j^2) N\left(\boldsymbol{x}, \boldsymbol{\mu_{jx}}, \delta_{jxx}\right) \\ m_j(\boldsymbol{x}) &= \mu_{jY} + \delta_{jYx}{\delta_{jx}}^{-1}\left(\boldsymbol{x} - \boldsymbol{\mu_{jx}}\right) \\ {\tau_j}^2 &= \delta_{jYY} - \delta_{jYx}{\delta_{jx}}^{-1}\delta_{jxY} \end{aligned} \tag{5}$$

Based on the partitioned format of Gaussian mixture density function, marginal density of $\boldsymbol{x}$ and conditional density of $y|\boldsymbol{x}$ can be formulated as Eqs. (6) and (7).

$$f(\boldsymbol{x}) = \sum_{j=1}^{k} \pi_j N\left(\boldsymbol{x}, \boldsymbol{\mu_{jx}}, \delta_{jxx}\right) \tag{6}$$

$$f(y|\boldsymbol{x}) = \sum_{j=1}^{k} w_j(\boldsymbol{x}) N(y|\boldsymbol{x}, m_j(\boldsymbol{x}), \tau_j^2) \tag{7}$$

Where $w_j(\boldsymbol{x})$ is the weight of each regression model and can be extracted using Bayes' rule shown in Eq. (8).

$$w_j(\boldsymbol{x}) = \frac{\pi_j N\left(\boldsymbol{x}; \boldsymbol{\mu_{jx}}, \delta_{jx}\right)}{\sum_{j=1}^{k} \pi_j N\left(\boldsymbol{x}; \boldsymbol{\mu_{jx}}, \delta_{jx}\right)} \tag{8}$$

Given the input data, GMMR provides mean value $\hat{y}(\boldsymbol{x})$ of output prediction using Eq. (9).

$$\hat{y}(\boldsymbol{x}) = E[Y|\boldsymbol{X} = \boldsymbol{x}] = \sum_{j=1}^{k} w_j(\boldsymbol{x}) m_j(\boldsymbol{x}) \tag{9}$$

4. UKF-GMMR

Due to change in system performance resulting from changes in operating conditions, parameters of system model should be modified accordingly. A UKF algorithm has been considered to update the model parameters $\boldsymbol{\theta}$ according to change in dynamic of the system. As mentioned in Eq. (10), parameter vector which is considered to be adjusted by UKF includes mean values of output data clusters.

$$\boldsymbol{\theta} = [\mu_{1Y,\ldots,}\ \mu_{kY}]^{\mathbb{T}} \tag{10}$$

The state space representation for parameter estimation of a dynamic system with process noise e_T^p and measurement noise e_T^m is shown in Eq. (11).

$$\begin{aligned} \boldsymbol{\theta}[T+1] &= \boldsymbol{\theta}[T] + e_T^p \\ y[T] &= h\left(\boldsymbol{x}[T], \boldsymbol{\theta}[T]\right) + e_T^m \end{aligned} \tag{11}$$

Where T is time step and output mapping function h shown in Eq. (12) is the GMMR resulted from combining Eqs. (8) and (9).

$$h\left(\boldsymbol{x}, \boldsymbol{\theta}\right) = \sum_{j=1}^{k} \frac{\pi_j N\left(\boldsymbol{x}; \boldsymbol{\mu_{jx}}, \delta_{jx}\right)}{\sum_{j=1}^{k} \pi_j N\left(\boldsymbol{x}; \boldsymbol{\mu_{jx}}, \delta_{jx}\right)} \left[\mu_{jY} + \delta_{jYx}{\delta_{jx}}^{-1}\left(\boldsymbol{x} - \boldsymbol{\mu_{jX}}\right)\right] \tag{12}$$

The UKF starts by defining initial values for parameters vector, Eq. (13), and parameters estimation error covariance matrix, Eq. (14) [38].

$$\hat{\boldsymbol{\theta}}_0^+ = E\left[\boldsymbol{\theta}_0\right] \tag{13}$$

$$P_{\theta_0}^+ = E\left[(\boldsymbol{\theta}_0 - \hat{\boldsymbol{\theta}}_0^+)(\boldsymbol{\theta}_0 - \hat{\boldsymbol{\theta}}_0^+)^{\mathbb{T}}\right] \tag{14}$$

Time update Eqs. (15) and (16) propagates covariance and parameter estimation from time step $(T-1)$ to time step T. Based on state space representation, the best value for vector of parameters in time step T and before observing measurement, is the value estimated in time step $(T-1)$ with added process noise covariance $R_{T-1}^p = E[e_{T-1}^p (e_{T-1}^p)^{\mathbb{T}}]$.

$$\hat{\boldsymbol{\theta}}_{\boldsymbol{T}}^- = \hat{\boldsymbol{\theta}}_{\boldsymbol{T}-1}^+ \tag{15}$$

$$P_{\theta_T}^- = P_{\theta_{T-1}}^+ + R_{T-1}^p \tag{16}$$

Given the estimated parameters, nonlinear GMMR function predicts the measurement in time step T using Eq. (17).

$$\hat{y}_T = h\left(\boldsymbol{x}_T, \hat{\boldsymbol{\theta}}_T^-\right) \tag{17}$$

Once measurement y_T at time step T arrives, we can update parameters estimation $\hat{\boldsymbol{\theta}}_T^+$ and covariance error matrix $\hat{P}_{\theta T}^+$ using Eqs. (18) and (19).

$$\hat{\boldsymbol{\theta}}_T^+ = \hat{\boldsymbol{\theta}}_T^- + K_g\left(y_T - \hat{y}_T\right) \tag{18}$$

$$\hat{P}_{\theta T}^+ = P_{\theta_T}^- - K_g P_y {K_g}^{\mathbb{T}} \tag{19}$$

The Kalman gain K_g and the measurement prediction covariance P_y are computed using unscented transformation. Appendix B elaborates the usage of unscented transformation in parameter estimation.

5. Case study for a chiller plant

5.1. System model and data collection

An all-variable speed water-cooled chiller plant located in Berkeley, California, is used as a case study to evaluate the AGMM fault detection and diagnosis algorithm. Fig. 2 depicts the system diagram of chilled water and condensing water loop. The system main components entail three parallel-coupled dissimilar chillers ARU1, ARU2 and ARU3 with nominal cooling capacities of 200 ton, 325 ton, and 60 ton, respectively, three air handler units AHU1, AHU2 an AHU3 and one cooling tower enfolding two similar cells CT01 and CT02. Chillers individually are equipped with one pump responsible for circulating chilled water and another pump assigned to move condenser water. In current version of the chiller plant, the chilled water and condenser water pumps in primary loop operate at constant speed. Additionally, a pump is allocated to maintain the pressure drop in the secondary loop. The speed of secondary loop pump is correlated with the chiller stage. Table 1 summarizes the information of chillers and associated pumps.

The control operation strategies of the chiller plant were adopted based on the actual control operation strategies of the real

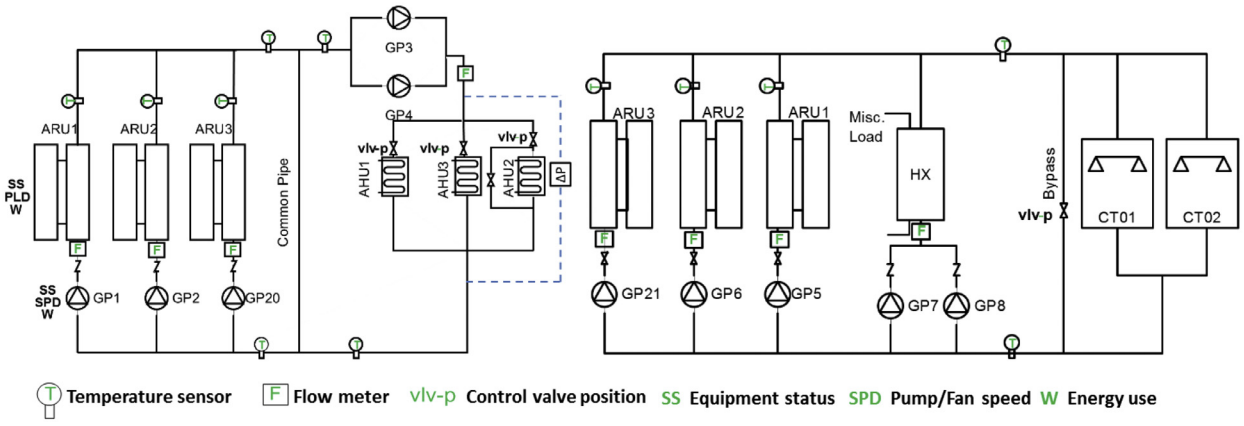

Fig. 2. Chiller plant configuration [39].

Table 1
Chiller plant information.

Chiller	Capacity (ton)	Design condition				Chilled water Pumps		Condenser water pumps	
		chilled water supply temperature (°C)	chilled water return temperature (°C)	Chilled water flow rate (kg/s)	Condenser water flow rate (kg/s)	Power (kW)	Flow rate (kg/s)	Power (kW)	Flow rate (kg/s)
ARU1	200	7.2	15.5	20.2	32	3.5	31.9	7.3	46.7
ARU2	325	7.2	15.5	32.8	51.5	3.9	31.6	12.5	65.5
ARU3	60	7.2	15.5	5.7	10.2	1.1	9.7	2.1	13.5

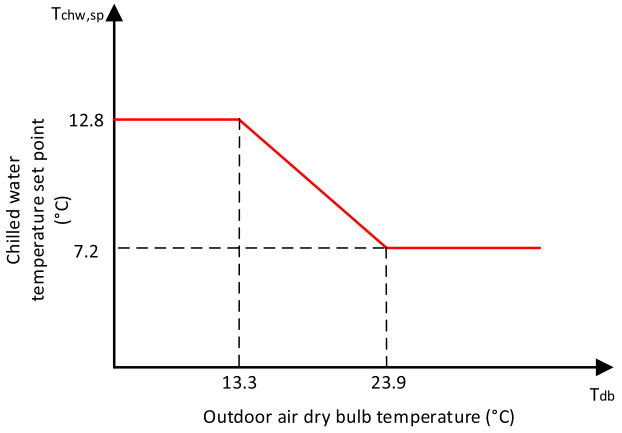

Fig. 3. Supply chilled water temperature reset strategy [40].

chiller plant. Condensing water temperature setpoint is 18.6 °C. The chilled water temperature setpoint reset is based on the outdoor air dry bulb temperature. Fig. 3 shows the implemented chilled water temperature reset strategy.

The chiller sequencing control is performed based on the outdoor air dry bulb temperature and cooling load. Five stages, stages 0 to 4, are defined for operation of the chiller plant. The stage 0: all the chillers are off, the stage 1: only chiller ARU3 is on, the stage 2: only chiller ARU1 is on, the stage 3: only chiller ARU2 is on, the stage 4: both chillers ARU1 and ARU2 are on.

The cooling tower staging control is linked to the chiller stage. For chiller stages 0 and 1, one cooling tower is used while for chiller stages 2–4, two cooling towers are activated to satisfy the condenser water temperature setpoint. In each cooling tower, a PID controller is designed to adjust the fan speed based on the error between the cooling tower leaving water temperature and the condenser water temperature setpoint.

Table 2
Information of secondary chilled water pump.

Chiller plant stage	Secondary chilled water pump		
	Power (kW)	Flow rate (kg/s)	DP setpoint (bar)
Stage 1	0.023	6.6	0.11
Stage 2	0.95	23.5	0.38
Stage 3	4	37.6	0.62
Stage 4	4.2	38.7	0.62

The secondary loop pump control system incorporates a PID controller to maintain the pressure difference setpoint in the secondary loop by adjusting the pump speed. The pressure difference set point is reset according to the chiller plant stage. Each stage applies a constant pressure difference set point. Table 2 shows the information of secondary chilled water pump.

The chiller performance has been modeled using three performance curves for the chiller capacity, the chiller full load efficiency, and the chiller efficiency. The independent variables for the chiller available capacity and the chiller full load efficiency curves are chilled water and condenser water supply temperature. The chiller efficiency is explained as a function of chiller part load ratio. We also used a regression model to simulate the load as a function of outdoor air dry bulb temperature.

For a primary-secondary water-cooled chiller plant, major energy consumers are chillers, primary pumps, secondary pumps, condensing water pumps, and cooling towers fans. The chiller power consumption is defined as a function of chilled water supply temperature, condenser water supply temperature, chilled wa-

ter return temperature, chiller partial load, and chiller nominal capacity.

A comprehensive physic based model of the multi-chiller plant has been developed and calibrated [39]. More details of the chiller plant model and the equations corresponding to the power consumption can be found in [40]. This model is used as the reference in lieu of real system to generate training and test data.

5.2. Model performance evaluation criteria

Five indices, namely, Root Mean Squared Error (RMSE) described in Eq. (20), Cumulative Variation of Root Mean Square Error (CVRMSE) described in Eq. (21), Normalized Mean Bias Error (MBE) described in Eq. (22), Maximum Absolute Error (MAE) Eq. (23), and Maximum Absolute Relative Error (MARE) Eq. (24) are used to evaluate the performance of different models.

$$RMSE = \sqrt{\frac{\sum_{T=1}^{N}\left(y[T]-\hat{y}[T]\right)^2}{N}} \tag{20}$$

$$CVRMSE = \frac{\sqrt{\frac{\sum_{T=1}^{N}\left(y[T]-\hat{y}[T]\right)^2}{N-1}}}{\bar{y}} \times 100 \tag{21}$$

$$NMBE = \frac{\frac{\sum_{T=1}^{N}\left(y[T]-\hat{y}[T]\right)}{N-1}}{\bar{y}} \times 100 \tag{22}$$

$$MAE = \max_{T}\left(\left|y[T]-\hat{y}[T]\right|\right) \tag{23}$$

$$MARE = \max_{T}\left(\left|\frac{y[T]-\hat{y}[T]}{y[T]}\right|\right) \tag{24}$$

where N is the number of observations, $y[T]$ is measured value at time step T, $\hat{y}[T]$ is predicted value at time step T, and $\bar{y}$ is the average of measured value.

5.3. UKF-GMMR model for chiller plant

The simulation of chiller plant Dymola model is conducted with 10 min time interval for one month in May to collect data for training the GMMR model. The 10 min time interval is chosen to be consistent with the measurement sampling rate at the real chiller plant. The month of May has been chosen to simulate training data since all possible operational modes of chiller plant have been covered. The collected data include outdoor air dry bulb temperature (T_{db}), wet bulb temperature (T_{wb}), chilled water supply temperature ($T_{chw,\,s}$), and chilled water return temperature ($T_{chw,\,r}$) as input data ($\boldsymbol{x}$) and total power consumption (P_{tot}) as output data ($\boldsymbol{y}$).

$$\boldsymbol{x} = \left[T_{db},\ T_{wb},\ T_{chw,s},\ T_{chw,r}\right]^{\mathbb{T}} \tag{25}$$

$$\boldsymbol{y} = P_{tot} \tag{26}$$

In this section, we develop a time-varying model for prediction of total power consumption in chiller plant, based on UKF-GMMR approach. The performance of UKF-GMMR model is compared with autoregressive exogenous (ARX) and recursive least square autoregressive exogenous (RLS-ARX) models as well [41]. Given training input and output data, Genetic optimization algorithm recognizes the optimal order of ARX model which gives minimum Bayesian information criteria (BIC) as an objective function. The same ARX model is employed in the RLS-ARX model.

Training GMMR model requires setting the number of mixture clusters in advance. A low number of components leads to poor accuracy. However, it has been shown that unnecessary increasing the number of components can over-fit the data and provides singularity in process of likelihood maximization [7]. Singularity problem prevents EM method from convergence to appropriate mixture model. RMSE criterion determines the optimal number of components in GMMR model. Keeping the same training data, the number of components is increased gradually. Once there is no significant improvement in RMSE value, the associated number of components is considered as optimal value. For this study, as illustrated in Fig. 4, no further reduction is observed for the number of components bigger than $k = 8$. Components weight, mean and covariance matrix, as parameters of GMMR model, are determined using EM algorithm. Same GMMR model is employed in the UKF-GMMR method. Degradation faults were detected and diagnosed based on the variation of the key parameter μ_{jY} of each Gaussian component in the UKF-GMMR model predicting electricity demands of the chiller plant. Eq. (27) shows the parameter vector which is considered to be adjusted by UKF.

$$\boldsymbol{\theta} = [\mu_{1\mathrm{Y},\ldots,}\ \mu_{8\mathrm{Y}}]^{\mathbb{T}} = [\mathrm{GMMR}\mu 1, \ldots,\ \mathrm{GMMR}\mu 8]^{\mathbb{T}} \tag{27}$$

As illustrated in Table 3, amongst proposed methods, ARX model with RMSE of 165.64 KW offers the lowest accuracy in predicting chiller plant total power. One reason for the low performance of ARX model could be fitting a linear structured model to a nonlinear system. Along with linearization error, there are some dynamics in evaluation data which has not appeared in training set of data. Employing recursive least square method to adjust ARX model parameters improves accuracy in RLS-ARX model with RMSE as 23.62 KW. RLS can track slow changes in the system. As shown in Fig. 5, there are still problems in predicting the transition points. Although RLS-ARX model is acceptable according to ASHRAE standard [38], it gives a weak prediction for fault detection applications due to high values of MAE as 110.97 KW and MARE as 3.04. The RLS-ARX provides large MAE when there is a change in the chiller stage. The values of prediction error are considerably high at the beginning of the simulation. GMMR model cannot appropriately predict the system output when systems operation condition changes or the system experiences faulty opera-

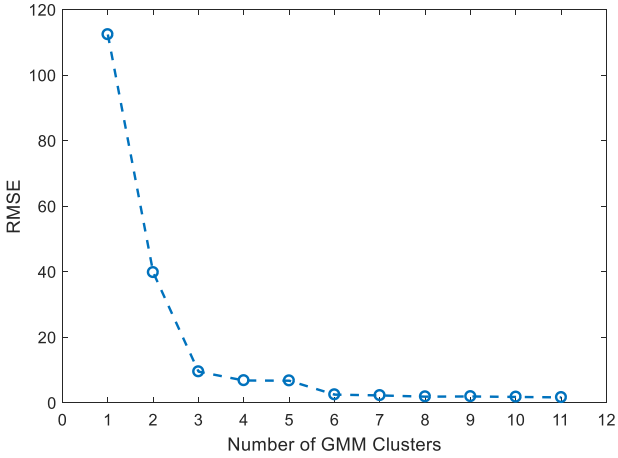

Fig. 4. Variation of RMSE as function of number of clusters in GMM.

Table 3
Prediction accuracy of chiller plant total power in July.

Model	Performance Index				
	RMSE kw	CVRMS E%	NMBE %	MAE kw	MARE
ARX	165.64	19.45	0.03	35.77	0.99
RLS-ARX	23.62	7.34	0.15	110.97	3.04
UKF-GMMR	0.70	1.27	0.01	13.52	0.43

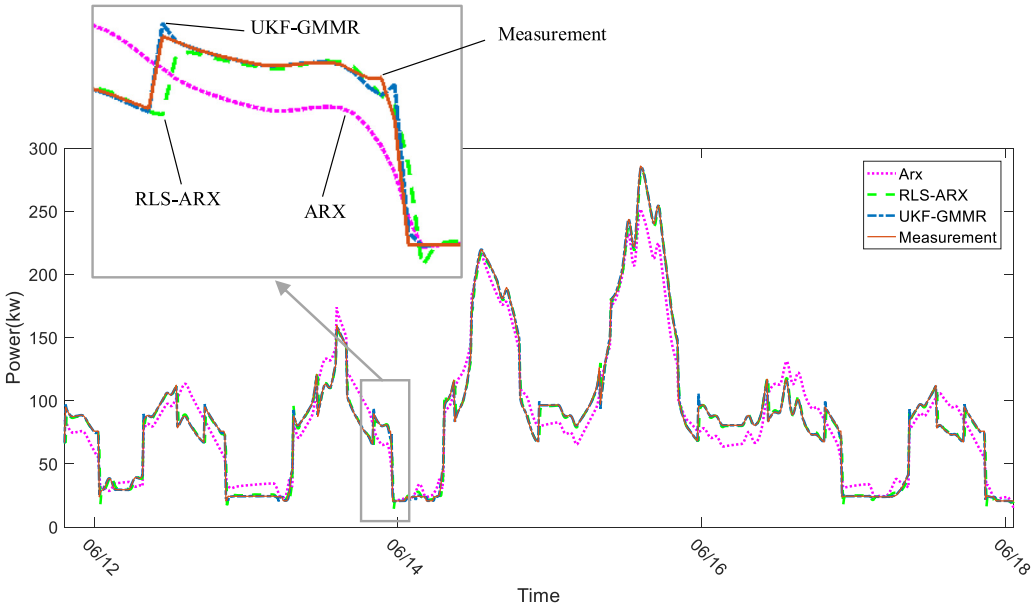

Fig. 5. Total power consumption prediction in chiller plant.

Table 4
Fault conditions in chiller plant.

Chiller plant component	Fault-free condition	Fault condition
Chiller 1	$COP_{nom} = 5.136$	$COP_f = 3.081$
Chiller 2	$COP_{nom} = 7.642$	$COP_f = 5.350$
Chiller 3	$COP_{nom} = 6.636$	$COP_f = 4.640$

tion. Integration of UKF with GMMR to have a nonlinear adaptive model, as demonstrated in Table 3, can end up with substantial improvement in prediction accuracy with RMSE as 0.70 KW. UKF-GMMR benefits from properties of both nonlinear modeling approaches and adaptive systems. There is also the minimum value for MAE among all methods which makes UKF-GMMR model reliable for fault detection applications. As illustrated in Fig. 5, the UKF-GMMR model provides an accurate prediction of the total power consumption even in the transition points when the chiller plant experiences a sudden change in its state.

5.4. Fault selection

Chillers account for a large amount of energy consumption in chiller plant. Energy efficiency of chillers could degrade over time. This can be reflected in the reduced nominal coefficient of performance (COP) of the chiller. Condenser fouling, evaporator fouling, and compressor motor degradation are major factors which reduce the chiller COP. Early detection of these faults provides considerable energy saving. In this paper, in order to simulate the faults, we changed the nominal COP of individual chillers which is a fixed parameter and part of chiller properties. Table 4 shows chiller plant parameters for fault-free and faulty conditions. It is assumed that chillers faults are not severe and chilled water temperature set-point can still be met in presence of the faults. The faults only change the energy consumption in the system.

5.5. Fault diagnosis training

Using fault-free test data, we extract a baseline for GMMR parameters. We define a threshold for each parameter based on three standard deviations from its mean value of fault-free conditions. Table 5 shows the threshold value for each GMMR parameter. Once baseline and threshold for each parameter are defined, one week of faulty operation data is used to extract fault diagnosis rules.

Fault in chiller 1: One week of test data has been used to study the effect of the faulty operation of chiller 1 on GMMR parameters. For this purpose, COP of chiller 1 has been dropped from 5.136 to 3.081 in Chiller plant model and faulty operation of chiller 1 continues for one week, then it is set back to normal operation. As demonstrated in Fig. 6, comparison of simulation result between faulty chiller 1 and fault-free condition, shows a significant increase in GMMRμ6. There is no change in rest of parameters over the time period of chiller 1 faulty operation. Therefore, monitoring of parameter GMMRμ6 through chiller plant operation provides adequate information to detect energy efficiency fault in chiller 1.

Fault in chiller 2: In this case, the operation of chiller plant is affected by energy efficiency fault in chiller 2. COP of chiller 2 has been reduced from 7.642 to 5.350 for one week leading the chiller 2 to operate under moderate faulty condition. Simulation results are shown in Fig. 7. As shown in Fig. 7(d) and (e), GMMRμ4 and GMMRμ5 parameters increase due to fault in chiller 2. Changes in parameters were observed once the chiller 2 is turned on. Since no change in other parameters was observed, tracking the GMMRμ4 and GMMRμ5 can reveal the abnormal operation of chiller 2.

Fault in chiller 3: In this case, faulty operation of chiller 3 is considered. To impose fault on the energy efficiency of chiller 3, nominal COP of this chiller is reduced from 6.636 to 4.640 for one week. In chiller plant under study, chiller 3 has low capacity and its operation accounts for a small portion of total energy consumption in chiller plant. Therefore, detecting moderate energy efficiency in this chiller is a hard task. Fig. 8 shows simulation result in the case of chiller 3 faulty operation. It can be observed from Fig. 8(c) and (g) that GMMRμ3 and GMMRμ7 are affected by a fault in chiller 3. It implies that GMMR model has devoted two clusters to explain the behavior of chiller 3. It is justifiable since in our chiller plant two modes of operation have been defined for chiller 3 operation. In some cases, when the cooling load is relatively low and just chiller 3 is active, control system turns off the cooling tower fan. Parameter GMMRμ7 is pertinent to this cluster of operation which rarely happens in our system. Therefore, we focus more on GMMRμ3 to detect and diagnose the fault in chiller 3.

Table 5
Thresholds for GMMR parameters.

	GMMRμ1	GMMRμ2	GMMRμ3	GMMRμ4	GMMRμ5	GMMRμ6	GMMRμ7	GMMRμ8
Threshold(kW)	–	167.8 178	20.79 33.95	93.5 108.6	76.36 83.2	82.5 100	17.42 24.21	–

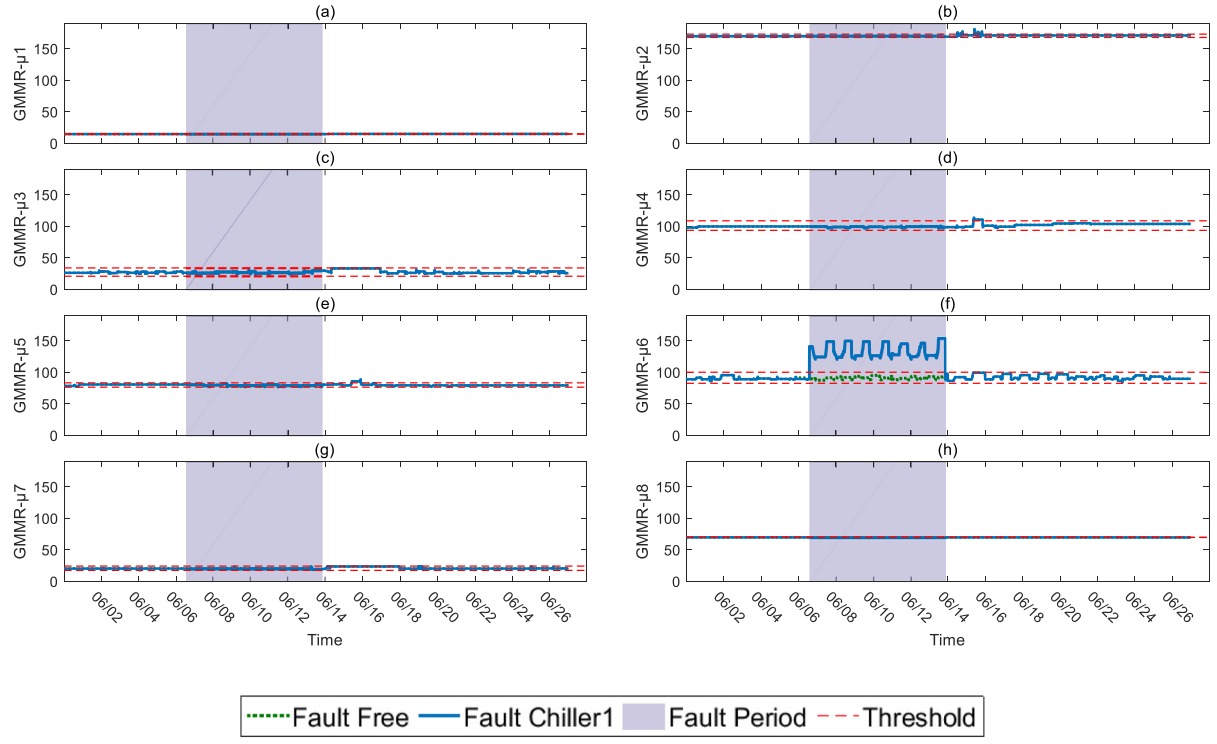

Fig. 6. Gaussian mixture parameters monitoring for the case of fault in chiller 1.

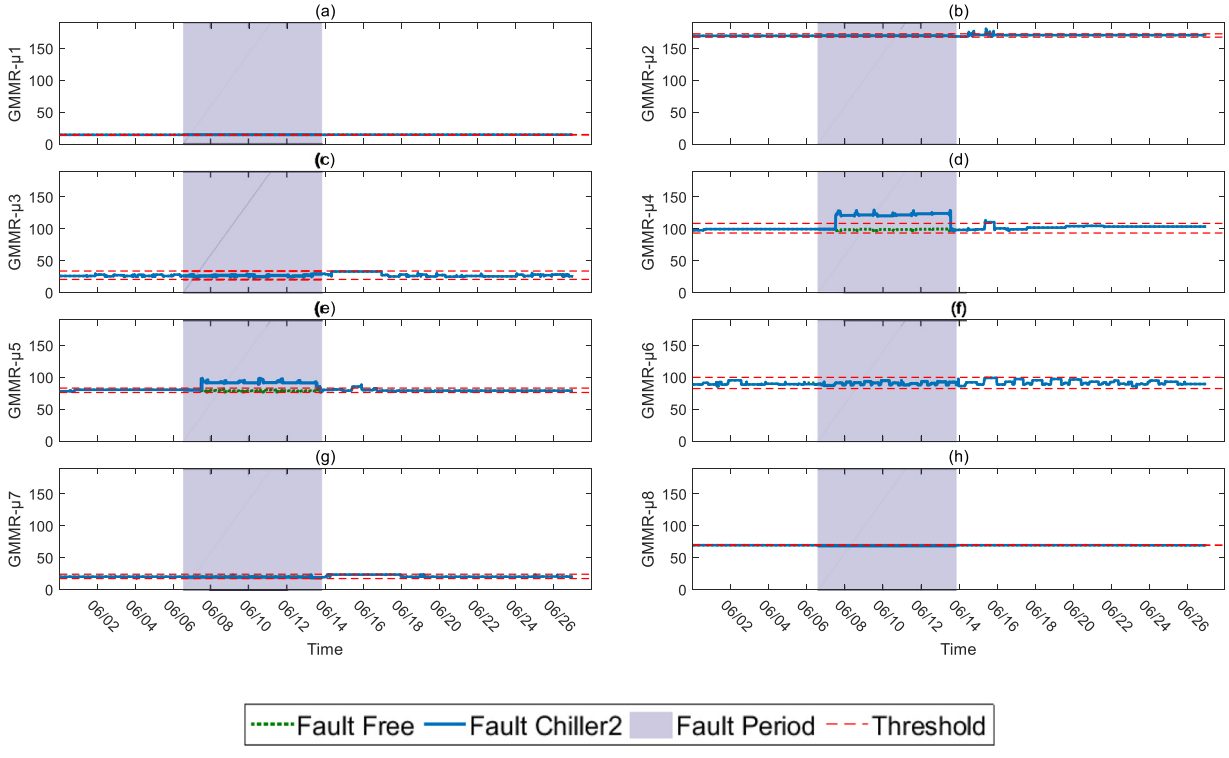

Fig. 7. Gaussian mixture parameters monitoring for the case of fault in chiller 2.

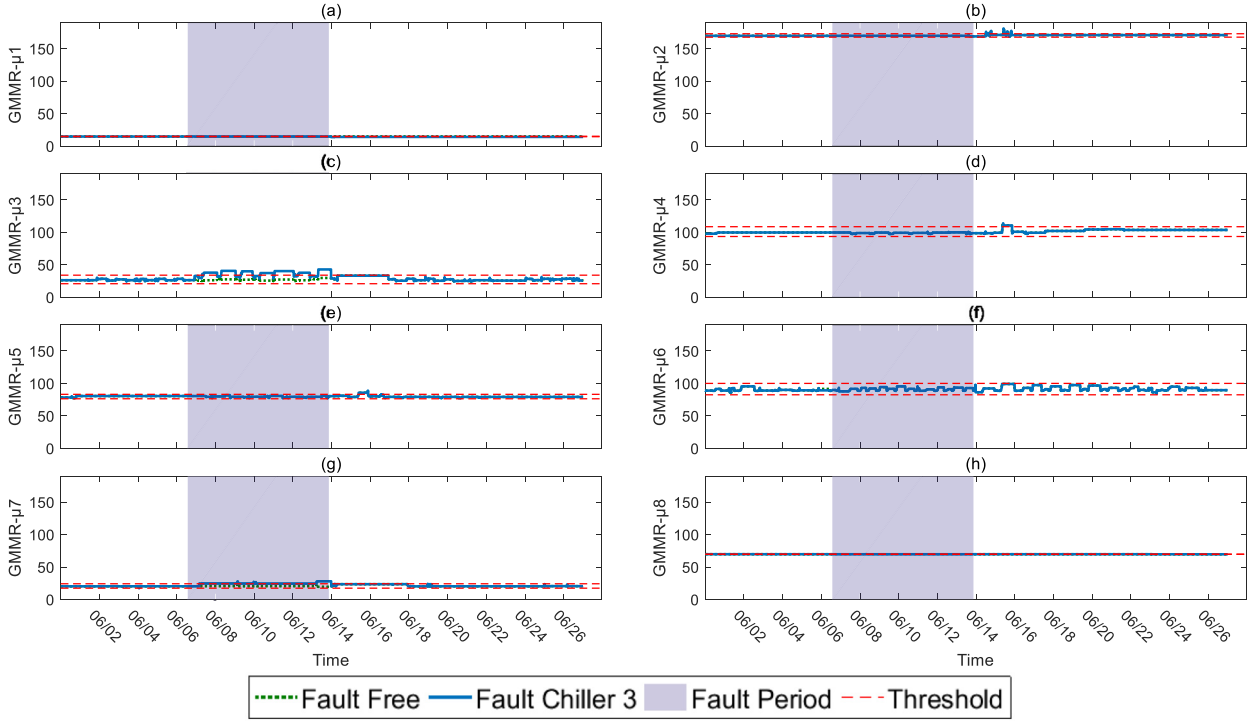

Fig. 8. Gaussian mixture parameters monitoring for the case of fault in chiller 3.

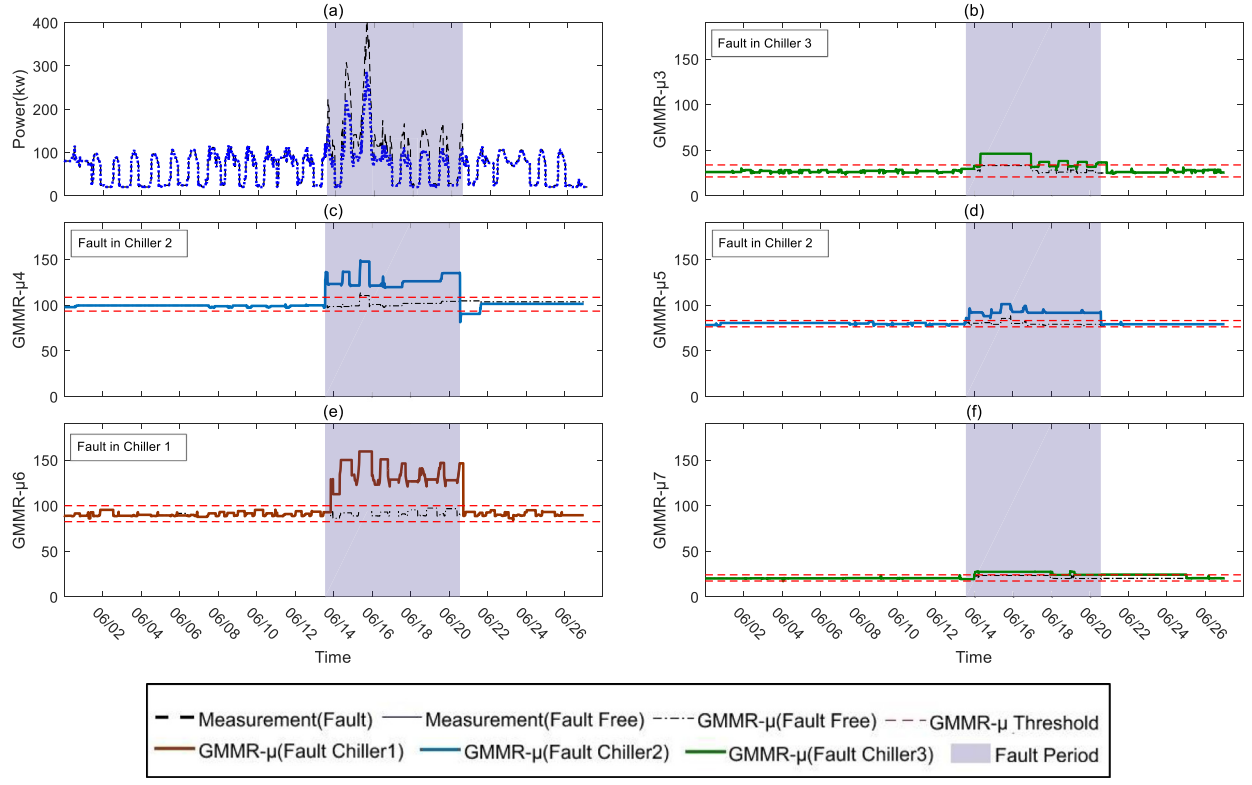

Fig. 9. Gaussian mixture parameters monitoring using test data.

Table 6 concludes diagnosis rules extracted from analyzing the influence of separate faults on the variation of GMMR parameters. Given the new data, diagnosis rules detect the possible fault in chiller plant system.

5.6. Testing AGMM algorithm

To evaluate the performance of the proposed AFDD algorithm, a set of input-output data corresponding to unlabeled faults in chiller plant is introduced to the algorithm. The separate time period compared to that used to train the AFDD algorithm and gen-

Table 6
General rules for energy efficiency fault detection and diagnosis in chiller plant.

	GMMRμ1	GMMRμ2	GMMRμ3	GMMRμ4	GMMRμ5	GMMRμ6	GMMRμ7	GMMRμ8
Chiller1 Energy fault	–	–	–	–	–	↑	–	–
Chiller2 Energy fault	–	–	–	↑	↑	–	–	–
Chiller3 Energy fault	–	–	↑	–	–	–	–	–

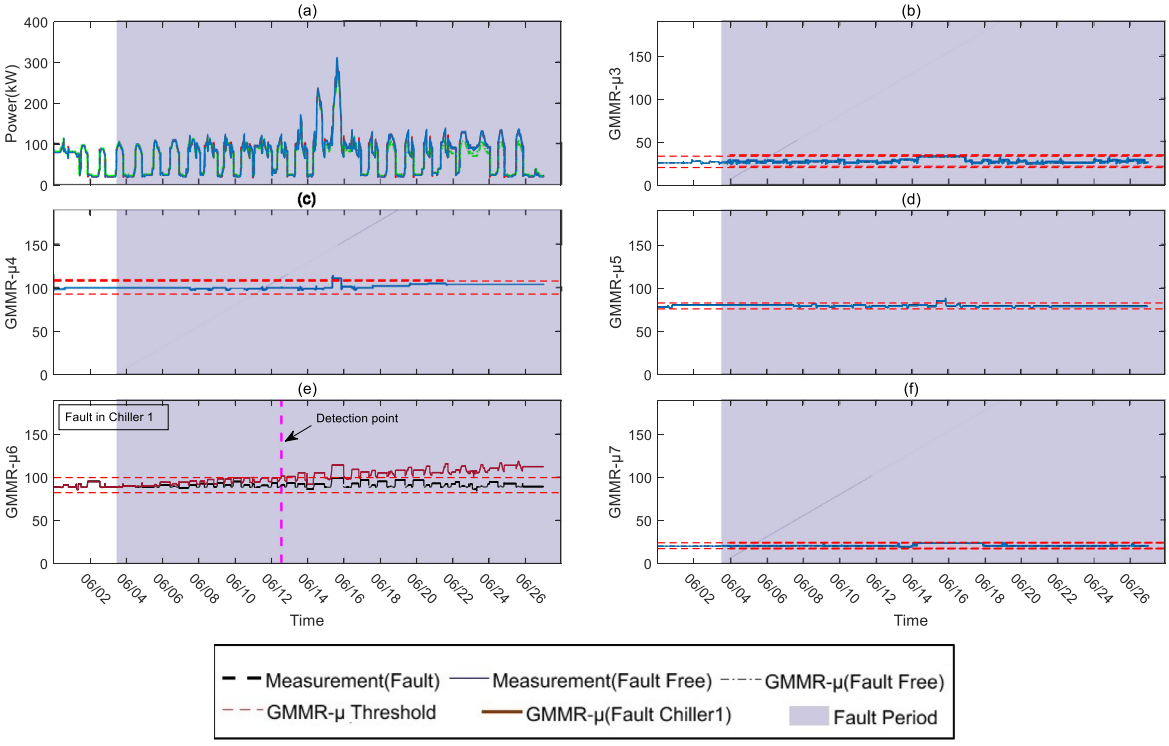

Fig. 10. Detection of incremental fault using AGMM.

erate the rules in Table 6, is used to assess the AFDD algorithm. Fig. 9 shows variation in total power consumption and GMMR parameters.

As shown in Fig. 9(a), total power consumption in chiller plant has been increased compared to power consumption in fault-free condition. However, no visible information can be captured to reveal the occurrence of the fault and associated faulty sub-component, merely by monitoring the power consumption. Fig. 9(b) demonstrates abnormal raise in violation from the threshold for parameter GMMRμ3. Referring to Table 6, chiller 3 is flagged as a faulty component. Rapid change in parameters GMMRμ4 and GMMRμ5, as shown in Fig. 9(c) and (d), indicates the occurrence of energy efficiency fault in chiller 2. As demonstrated in Fig. 9(e), a fault in chiller 1 is clearly detected as GMMRμ6 violates the threshold. Although faults occurred simultaneously, AGMM method could successfully detect and diagnosis all faults accurately.

The performance of the proposed AFDD algorithm for detecting and diagnosing incremental degradation of chiller performance is also evaluated. As an illustration, the energy efficiency of chiller 1 gradually degrades over the time to collect the test data. In this case, the COP of chiller 1 decreases from 5.136 to 3.600 in 24 days. Fig. 10 shows the result of the AFDD algorithm.

As shown in Fig. 10(e), GMMRμ6 starts to change when the energy efficiency of chiller 1 starts to degrade. Since the degradation increases slowly, after 9 days, GMMRμ6 exceeds the threshold and AFDD algorithm can detect the fault. It is found that the fault belongs to chiller 1 as the other parameters remain unchanged.

The simulation study demonstrates the success of the new method AGMM in detecting and diagnosing chiller performance degradation faults in the multi-chiller plant. The AGMM benefits from an unsupervised learning approach to model the multi-chiller plant system which reduces the modeling effort and meets the required accuracy in detection of both sudden and incremental faults.

6. Conclusion

This paper introduced a new AGMM approach that automatically detects and diagnoses faults in nonlinear systems. In this method, time-varying parameters in the GMMR model react to the emergence of different faults and can lead to successful fault diagnosis. The proposed method was demonstrated in detecting and diagnosing chillers performance degradation faults in a multi-chiller plant system. The case study for the multi-chiller plant indicates AGMM can successfully detect and diagnose the simultaneous faults.

This AFDD method can reduce the number of sensors needed to detect and diagnose common faults in chiller plant. This approach also reduces modeling effort by developing a data-driven UKF-GMMR model representing fault-free operation.

The data-driven modeling algorithm UKF-GMMR can accurately predict total power consumption in the multi-chiller plant with prediction RMSE of 0.70 KW. UKF-GMMR outperforms ARX and RLS-ARX models evaluated in this study.

It is worth noting that preliminary tests were limited to the chiller performance degradation faults. In future research, we will consider detection and diagnosis of additional faults in chiller plant such as a blockage in valves, control and energy faults in the cooling tower, and erroneous sensors. Moreover, the robustness of proposed AFDD algorithm in presence of noisy measurement will be considered. We will also evaluate proposed AGMM approach for fault detection and diagnosis in other HVAC systems.

Acknowledgement

This research was funded by School of Energy Resource at the University of Wyoming.

Appendix A. EM algorithm

A binary random variable $\boldsymbol{Z}$ as a k-dimensional latent variable is defined in which element z_k is 1 and other elements are 0. Using Bayes' rule in Eq. (28), we can compute $\beta(z_{nj})$ which is named responsibility function and gives the membership of mixture component k corresponding to observation [7].

$$\beta\left(z_{nj}\right) = \frac{\pi_j N(\boldsymbol{d_n}|\boldsymbol{\mu_j}, \delta_j)}{\sum_{j=1}^{k} \pi_j N(\boldsymbol{d_n}|\boldsymbol{\mu_j}, \delta_j)} \tag{28}$$

EM algorithm requires an initial value for parameters. Appropriate initialization can reduce the number of iterations to convergence and increase the accuracy of the approximation. A common method is using K-means clustering algorithm to provide an initial value for parameters in EM process. EM algorithm pursues following steps.

1) In expectation step (E-step), responsibility function mentioned in Eq. (28) is evaluated given the current value of parameters.
2) In maximization step (M-step), parameters are updated using Eqs. (29)–(31) based on the value of responsibility function.
3) Log-likelihood function is evaluated using updated parameters. If the convergence criterion is not satisfied, EM algorithm will be continued. More information about convergence criterion can be found in [7].

$$\boldsymbol{\mu_j^{t+1}} = \frac{\sum_{n=1}^{N} \beta\left(z_{nj}\right)\boldsymbol{d_n}}{\sum_{n=1}^{N} \beta\left(z_{nj}\right)} \tag{29}$$

$$\delta_j^{t+1} = \frac{\sum_{n=1}^{N} \beta\left(z_{nj}\right)(\boldsymbol{d_n} - \boldsymbol{\mu_j^{t+1}})(\boldsymbol{d_n} - \boldsymbol{\mu_j^{t+1}})^{\mathbb{T}}}{\sum_{n=1}^{N} \beta\left(z_{nj}\right)} \tag{30}$$

$$\pi_j^{t+1} = \frac{\sum_{n=1}^{N} \beta\left(z_{nj}\right)}{N} \tag{31}$$

where t shows the iteration step.

Appendix B. Unscented Kalman filter

Once measurement y_T at time step T arrives, measurement update for system parameters is computed using sigma points and deploy unscented transformation. Eq. (32) shows sigma points $\hat{\boldsymbol{\theta}}_T^{(i)}$ based on the current best guess for parameters which is $\hat{\boldsymbol{\theta}}_T^{-}$.

$$\begin{aligned}
&\hat{\boldsymbol{\theta}}_T^{(i)} = \hat{\boldsymbol{\theta}}_T^{-} + \tilde{\boldsymbol{\theta}}^{(i)} \qquad i = 1, \ldots, 2k \\
&\tilde{\boldsymbol{\theta}}^{(0)} = 0 \\
&\tilde{\boldsymbol{\theta}}^{(i)} = \left(\sqrt{\gamma P_{\theta_T}^{-}}\right)_i \qquad i = 1, \ldots, k \\
&\tilde{\boldsymbol{\theta}}^{(i+L)} = -\left(\sqrt{\gamma P_{\theta_T}^{-}}\right)_i \qquad i = 1, \ldots, k \\
&\gamma = \alpha^2(k + \varphi)
\end{aligned} \tag{32}$$

where constants α and φ are small positive scaling factors and k is the dimension of parameter vector [20]. The square root of $P_{\theta_T}^{-}$, estimation error covariance matrix, can be computed taking advantage of Cholesky decomposition algorithm. As shown in Eq. (33), using GMMR function sigma points are transferred to measurement space.

$$\hat{y}_T^{(i)} = h\left(\boldsymbol{x}_T, \hat{\boldsymbol{\theta}}_T^{(i)}\right) \tag{33}$$

Eqs. (34) and (35) compute covariance of measurement prediction and cross-covariance between $\hat{\boldsymbol{\theta}}_T^{-}$ and $\hat{y}_T$ using transformed sigma points and predicted measurement at time step T. Measurement noise covariance R_T^m is added to measurement prediction covariance P_y.

$$\begin{aligned}
&P_y = \sum_{i=0}^{2k} W_c^{(i)}\left(\hat{y}_T^{(i)} - \hat{y}_T\right)\left(\hat{y}_T^{(i)} - \hat{y}_T\right)^{\mathbb{T}} + R_T^m \\
&W_c^{(0)} = \left(2 - \alpha^2 + \omega\right) - \frac{k}{\alpha^2(k + \varphi)} \\
&W_c^{(i)} = \frac{1}{2\alpha^2(k + \varphi)} \qquad i = 1, \ldots, 2k
\end{aligned} \tag{34}$$

$$P_{\theta y} = \sum_{i=0}^{2k} W_c^{(i)}\left(\hat{\boldsymbol{\theta}}_T^{(i)} - \hat{\boldsymbol{\theta}}_T^{-}\right)\left(\hat{y}_T^{(i)} - \hat{y}_T\right)^{\mathbb{T}} \tag{35}$$

In Eq. (34), ω represents the effect of prior knowledge about parameter distribution [20]. For Gaussian distribution, $\omega = 2$ is used in Eq. (34).

Eq. (36) accounts for measurement update of parameters estimation and error covariance matrix at time step T.

$$\begin{aligned}
&K_g = P_{\theta y} P_y^{-1} \\
&\hat{\boldsymbol{\theta}}_T^{+} = \hat{\boldsymbol{\theta}}_T^{-} + K_g\left(y_T - \hat{y}_T\right) \\
&\hat{P}_{\theta T}^{+} = P_{\theta_T}^{-} - K_g P_y K_g^{\mathbb{T}}
\end{aligned} \tag{36}$$

References

[1] S. Katipamula, M.R. Brambley, M.R. Brambley, Review article : methods for fault detection, diagnostics, and prognostics for building systems—a review, Part I, HVAC&R Res. 11 (1) (2005) 3–25.
[2] V. Venkatasubramanian, R. Rengaswamy, K. Yin, A review of process fault detection and diagnosis Part I: quantitative model-based methods, Comput. Chem. Eng. 27 (2003) 293–311.
[3] V. Venkatasubramanian, R. Rengaswamy, S.N. Ka, A review of process fault detection and diagnosis Part III: process history based methods, Comput. Chem. Eng. 27 (2003).
[4] V. Venkatasubramanian, R. Rengaswamy, S.N. Ka, A review of process fault detection and diagnosis Part II: qualitative models and search strategies, Comput. Chem. Eng. 27 (2003) 313–326.
[5] S. Katipamula, MichaelR. Brambley, Review article : methods for fault detection, diagnostics, and prognostics for building systems—a review, Part II, HVAC&R Res. 11 (2) (2005) 169–187.
[6] S. Wook, J. Hyun, I. Lee, Process monitoring using a Gaussian mixture model via principal component analysis and discriminant analysis, Comput. Chem. Eng. 28 (2004) 1377–1387.
[7] M. Bishop, Pattern Recognition and Machine Learning, Springer, 2006.
[8] H.G. Sung, Gaussian Mixture Regression and Classification PhD thesis, Rice University, Houston, Texas, 2004.
[9] B. Kolewe, A. Haghani, R. Beckmann, T. Jeinsch, Gaussian mixture regression and local linear network model for data-driven estimation of air mass, IET Control Theory Appl. 9 (7) (2015) 1083–1092.

[10] J. Lan, J.C. Principe, M.A. Motter, Identification of dynamical systems using GMM with VQ initialization, in: Neural Networks, Proc. Int. Jt. Conf. on, 1, 2003 1.
[11] C. Mei, Y. Su, G. Liu, Y. Ding, Z. Liao, Dynamic Soft sensor development based on Gaussian mixture regression for fermentation processes, Chin. J. Chem. Eng. 25 (1) (2017) 116–122.
[12] X. Yuan, Z. Ge, Z. Song, Soft sensor model development in multiphase / multimode processes based on Gaussian mixture regression, Chemom. Intell. Lab. Syst. 138 (2014) 97–109.
[13] G. Wang, L. Qian, Z. Guo, Continuous tool wear prediction based on Gaussian mixture regression model, Int. J. Adv. Manuf. Technol. 66 (2013) 1921–1929.
[14] S.M. Khansari-zadeh, A. Billard, Learning stable non-linear dynamical systems with Gaussian mixture models, IEEE Trans. Robot. 27 (5) (2011) 1–15.
[15] S. Calinon, A. Billard, A probabilistic programming by demonstration framework handling constraints in joint space and task space, in: IEEE/RSJ Int. Conf. Intell. Robot. Syst. Acrop. Conv. Cent., 2008, pp. 22–26.
[16] M. Fergie, A. Galata, Mixtures of Gaussian process models for human pose estimation, IMAVIS 31 (12) (2013) 949–957.
[17] M. Song, H. Wang, Highly efficient incremental estimation of gaussian mixture models for online data stream clustering, SPIE Conf. Intell. Comput. Theory Appl, 2005.
[18] A. Leonardis, M. Kristan, D. Skoc, Online kernel density estimation for interactive learning, Image Vis. Comput. 28 (2010) 1106–1116.
[19] O. Capp, E. Moulines, Online EM algorithm for latent data models, J. R. Stat. Soc. B 71 (3) (2007) 593–613.
[20] E.A. Wan, R. Van Der Merwe, N.W.W. Rd, The unscented kalman filter for nonlinear estimation, Adaptive Systems for Signal Processing, Communications, and Control Symposium. AS-SPCC, 2000.
[21] Y. Zhao, F. Xiao, S. Wang, An intelligent chiller fault detection and diagnosis methodology using Bayesian belief network, Energy Build. 57 (2013) 278–288.
[22] M. Najafi, D.M. Auslander, P.L. Bartlett, P. Haves, M.D. Sohn, Application of machine learning in the fault diagnostics of air handling units, Appl. Energy 96 (2012) 347–358.
[23] Y. Zhao, J. Wen, F. Xiao, X. Yang, S. Wang, Diagnostic Bayesian networks for diagnosing air handling units faults – Part I: faults in dampers, fans, filters and sensors, Appl. Therm. Eng. 111 (2017) 1272–1286.
[24] D. Dehestani, S. Su, H. Nguyen, Y. Guo, Robust fault tolerant application for HVAC system based on combination of online SVM and ANN black box model, in: European Control Conference, 2013, pp. 2976–2981.
[25] K. Yan, W. Shen, T. Mulumba, A. Afshari, ARX model based fault detection and diagnosis for chillers using support vector machines, Energy Build. 81 (2014) 287–295.
[26] A. Beghi, R. Brignoli, L. Cecchinato, G. Menegazzo, M. Rampazzo, F. Simmini, Data-driven fault detection and diagnosis for HVAC water chillers, Control Eng. Pract. 53 (2016) 79–91.
[27] S. kun Li, J. Wen, Application of pattern matching method for detecting faults in air handling unit system, Autom. Constr. 43 (2014) 49–58.
[28] D. Li, G. Hu, C.J. Spanos, A data-driven strategy for detection and diagnosis of building chiller faults using linear discriminant analysis, Energy Build. 128 (2016) 519–529.
[29] D. Li, Y. Zhou, G. Hu, C.J. Spanos, Fault detection and diagnosis for building cooling system with a tree-structured learning method, Energy Build. 127 (2016) 540–551.
[30] Q. Zhou, S. Wang, F. Xiao, Q. Zhou, S. Wang, A novel strategy for the fault detection and diagnosis of centrifugal chiller systems, HVAC&R Res. 15 (1) (2009) 57–75 ISSN.
[31] L. Wang, P. Haves, Monte Carlo analysis of the effect of uncertainties on model-based HVAC fault detection and diagnostics, HVAC&R Res. 20 (2014) 616–627.
[32] J. Yu, Engineering applications of artificial intelligence a new fault diagnosis method of multimode processes using Bayesian inference based Gaussian mixture contribution decomposition, Eng. Appl. Artif. Intell. 26 (1) (2013) 456–466.
[33] U. Thissen, H. Swierenga, A. P, R. Wehrens, W.J. Melssen, L.M.C. Buydens, Multivariate statistical process control using mixture modelling, J. Chemom. 19 (2005) 23–31.
[34] M. Bonvini, M.D. Sohn, J. Granderson, M. Wetter, M. Ann, Robust on-line fault detection diagnosis for HVAC components based on nonlinear state estimation techniques, Appl. Energy 124 (2014) 156–166.
[35] Q. Zhou, S. Wang, Z. Ma, A model-based fault detection and diagnosis strategy for HVAC systems, Int. J. Energy Res. 33 (2009) 903–918.
[36] R.L. Hu, J. Granderson, A. Agogino, Detection of chiller energy efficiency faults using expectation maximization, IDETC/CIE, 2015.
[37] M.C. Comstock, J.E. Braun, E.A. Groll, The sensitivity of chiller performance to common faults, HVAC&R Res. 7 (3) (2001) 263–279.
[38] D. Simon, Optimal State Estimation: Kalman, H Infinity, and Nonlinear Approaches, John Wiley and Sons Inc, 2006.
[39] L. Wang, S. Greenberg, M.A. Piette, A. Meier, J. Fiegel, Data analysis and modeling of an all- variable speed water-cooled chiller plant, ASHRAE Trans. 121 (2) (2015) 1.
[40] M. Karami, L. Wang, Particle swarm optimization for control operation of an all-variable speed water-cooled chiller plant, Appl. Therm. Eng. 130 (2018) 962–978.
[41] L. Ljung, System Identification: Theory for the User, Prentice-Hall PTR, Upper Saddle River, NJ, 1999.